Bull. Fac. Fish. Hokkaido Univ.
49(3), 107-116, 1998.

Numerical Simulation of the Formation of a Northward Deep Flow off Cape Henashi, Japan

Kosuke MORI[1] and Yutaka ISODA[1]

Abstract

Numerical simulations were carried out to investigate a possible cause of the observed steady northward deep flow (about 5.0 cm/s) off Cape Henashi, by using a two-dimensional barotropic model. Three different forces were used in the model: (1) inflow and outflow through the straits, (2) abyssal circulation due to wintertime convection, and (3) northwesterly constant wind in winter. Although each force induces northward flow off Cape Henashi, the steady flow cannot be reproduced throughout the year in cases (2) and (3), but only in wintertime. It seems therefore that the most probable cause of the steady constant deep flow of about 5.0 cm/s is the in- and outflow forces through the straits.

Key words: Japan Sea, Cape Henashi, Barotropic current, Two-dimensional model

Introduction

The Japan Sea is roughly 1,600 km long by 900 km wide with a maximum depth greater than 3,500 m. It is a semi-closed sea surrounded by the Japanese Islands, the Sakhalin, and the Asian Continent. It is connected to the China, Pacific and Okhotsk Seas only through shallow straits. Under the main thermocline, the water properties, which are called the Japan Sea Proper Water (JSPW), are nearly homogenous, with low temperature and salinity. Above JSPW, warm saline water entering through the Tsushima Strait flows northeastward, and most of it flows out through the Tsugaru and Soya Straits (Fig. 1).

Murakami et al. (1995) measured the current off Cape Henashi (40°36.6′N, 139°21.52′E, see Fig. 2) from April 2, 1994 through April 3, 1995. They revealed the structure of the Tsushima Warm Current by using the Aanderaa recording current meters. Two instruments were used: one was deployed at 300 m depth, the other at 2,100 m depth. Figure 3 shows the time series of the observed daily mean velocities at (a) 300 m depth and (b) 2,100 m depth. A steady pronounced northward flow was found at both depths. Their respective mean velocities were about 4.5 cm/s at 300 m depth and about 5.0 cm/s at 2,100 m.

As the northward flow off Cape Henashi can be considered to be nearly barotropic, it may be significant that a relatively strong flow exists even in deep water. A two-dimensional barotropic model was developed to investigate what causes barotropy of such northward flow. A model basin, which had the realistic bathymetry of the Japan Sea, was constructed to take account of the influence of the bottom relief.

[1] *Laboratory of Physical Oceanography, Faculty of Fisheries, Hokkaido University*
(北海道大学水産学部物理海洋学講座)

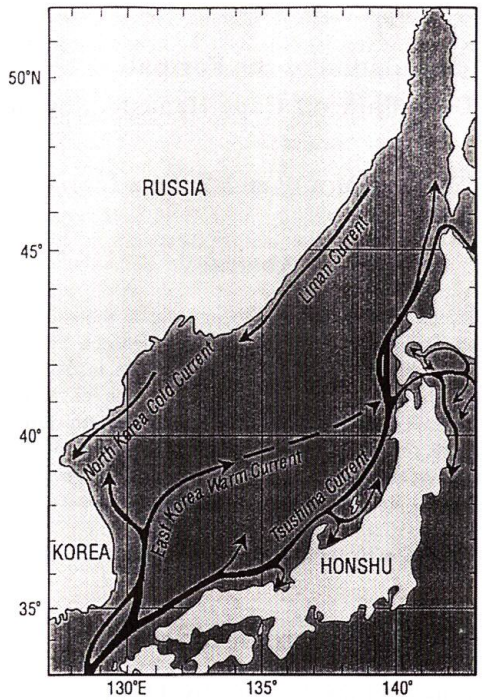

Fig. 1. Schematic view of the typical surface current paths in the Japan Sea (Holloway et al., 1995).

Numerical Model

Depth description

Figure 4(a) shows the bathymetry of the model basin used. The Japan Basin (e), the Yamato Basin (f), and the Tsushima Basin (g) are north, south, and southeast of the Yamato Rise (A1) and the Kita-Yamato Rise (A2) respectively. Figure 4(b) shows a contour map of (f/H) for the model topography. In general, the gradient of (f/H) is steep along the Asian Continent and the Japan Islands but is more gradual at the central part of the Japan Sea. Around the sea area off Cape Henashi, the topography β-effect is much larger than the planetary β-effect. This implies that the barotropic flow tends to follow the isobaths.

Equations

A rectangular coordinate system was used, taking x as eastward and y as northward. Let u and v be the components of velocity in the x and y directions respectively. The following linear equations of motion and continuity were used:

$$\frac{\partial u}{\partial t}-fv=-g\frac{\partial \eta}{\partial x}+A_h\left(\frac{\partial^2 u}{\partial x^2}+\frac{\partial^2 u}{\partial y^2}\right)-r_b\frac{u}{H} \tag{1}$$

$$\frac{\partial v}{\partial t}+fu=-g\frac{\partial \eta}{\partial y}+A_h\left(\frac{\partial^2 v}{\partial x^2}+\frac{\partial^2 v}{\partial y^2}\right)-r_b\frac{v}{H} \tag{2}$$

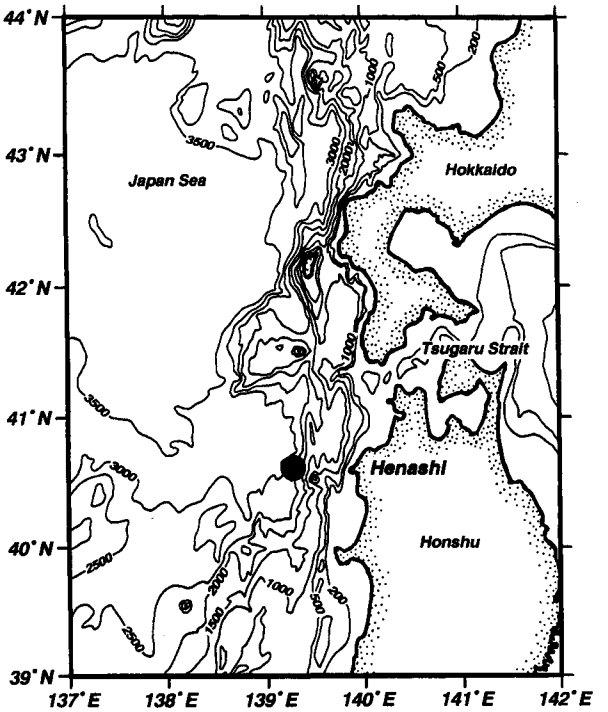

Fig. 2. Location of the observation station. The symbol ● indicates the deploying point of the direct current measurement.

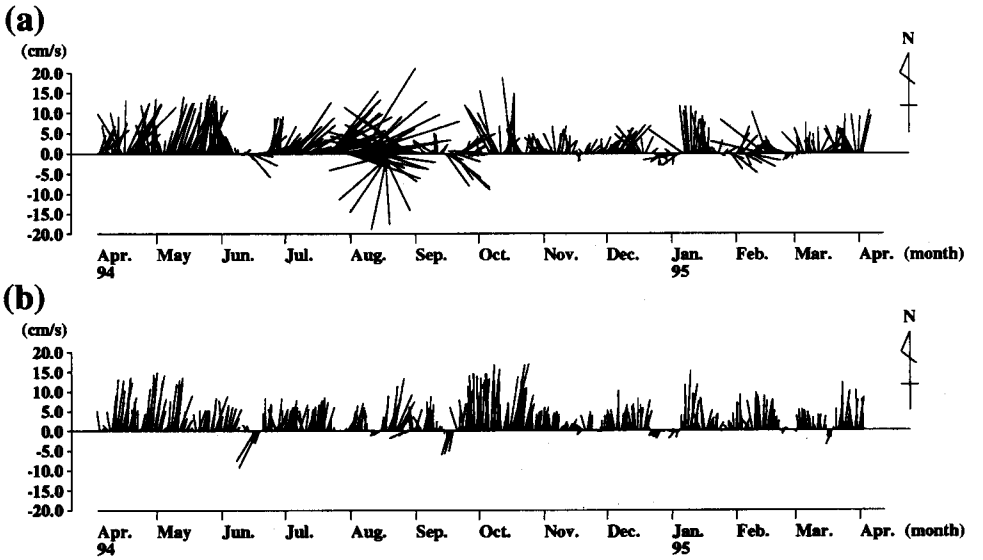

Fig. 3. Time series of the daily mean observed current at 300 m depth (a), and 2,300 m depth (b).

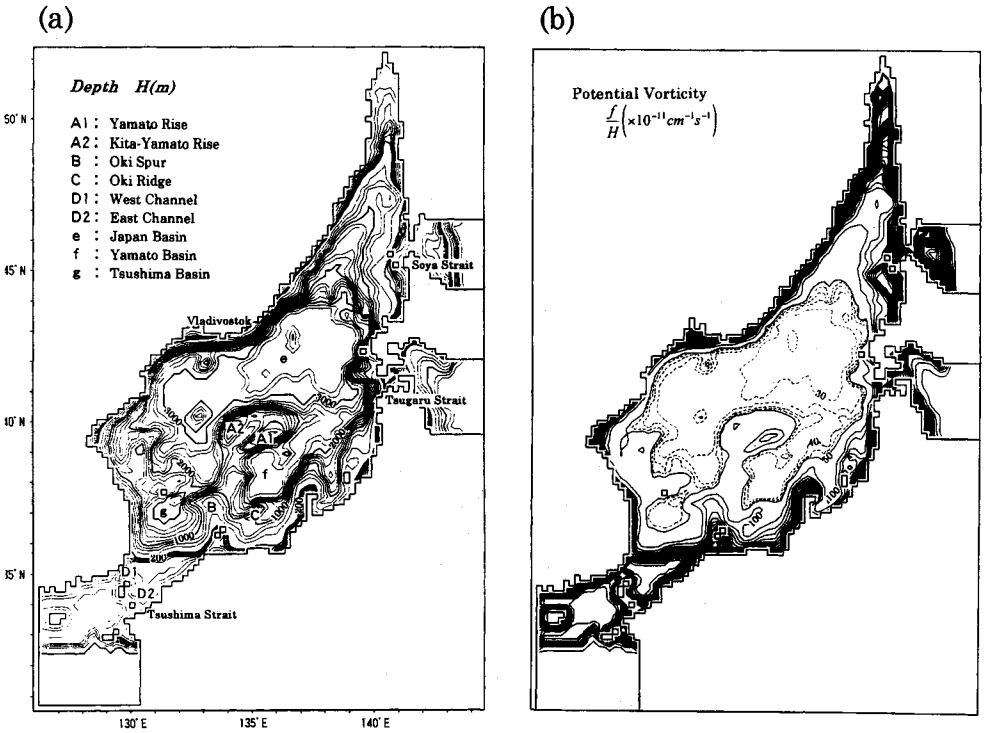

Fig. 4. Model domain with topography (a), and contours of constant (f/H) for the model topography (b). The contour intervals in (a) are 20 m for 0 m through 200 m and 200 m for greater than 200 m, and those in (b) are 5×10^{-11} $cm^{-1}s^{-1}$ (broken line) and 50×10^{-11} $cm^{-1}s^{-1}$ (solid line).

$$\frac{\partial\eta}{\partial t}+H\left(\frac{\partial u}{\partial x}+\frac{\partial v}{\partial y}\right)=0 \tag{3}$$

where η is the surface elevation, H is the depth, g is the gravity acceleration, and f is the Coriolis parameter. The coefficient of the horizontal eddy diffusion ($A_h=10^7$ cm^2/s) was fixed in all cases, whereas that of the bottom friction (r_b) had three different values ($r_b=0.1$, 0.01, and 0.001 cm/s), which were fixed in each individual case. These equations were solved numerically with a square grid resolution of 20 km.

Model cases

Three possible causes of the barotropic flow in the Japan Sea were considered.

Case 1. Inflow and outflow through the straits

As the Tsushima Warm Current is caused mainly by the pressure difference between the south of the Tsushima Strait and the east of the Tsugaru/Soya Strait, it was considered that the deep flow may also respond to this effect. In this case, inflow transport through the Tsushima Strait was taken to be constant at 2.0×10^{12} cm^3/s ($=2.0$ Sv). From the volume transport, the surface elevation at the southern

boundary of the reservoir outside the Tsushima Strait was estimated as

$$\frac{\partial \eta}{\partial t}=\frac{2.0}{L\Delta y}$$

where L is zonal length of the southern boundary and Δy is the grid resolution (= 20 km).

The boundary conditions at the eastern side of the reservoir outside the Tsugaru/Soya Strait are $\partial u/\partial x=0$ and $\eta=0$.

Case 2. Abyssal circulation due to wintertime convection

If the deep layer is much thicker than the surface one, it could be considered that the deep flow alone represents the barotropic flow almost exactly. In the Japan Sea, the thickness of the deep layer (3,500 m), i.e. JSPW, is much greater than that of the surface layer (300 m). Therefore, for a first approximation, the deep flow was assumed to be representative of the barotropic flow in the Japan Sea.

The model used in this case was the 1.5 layer (reduced gravity) model. Only the motion of the lower layer was considered and the upper layer was assumed to be infinite and motionless. Then, if g in eq. (1) is changed into g^*, the reduced gravity, g^* is assumed to be constant at 3.0 cm/s, taking account of the typical values of the Tsushima Warm Current water and the cold water beneath it.

As the depths of all straits in the Japan Sea are less than 150 m, the JSPW must be produced within the Japan Sea. For example, Senjyu and Sudo (1994) suggested from isopycnal analysis that the JSPW is formed by the wintertime convection in the region west of 136°E between 40° and 43°N. Using this suggestion, water from off Vladivostok was allowed to enter the model for 90 days, corresponding to the period of winter. The entering water mass transport is fixed at a constant value of 1.0 Sv. The boundary condition at the grid points adjacent to Vladivostok is

$$\frac{\partial \eta}{\partial t}=\frac{1.0}{S}$$

where S is the grid area corresponding to the water entering region.

When the coefficient of Newtonian damping λ is incorporated, eq. (3) is changed into

$$\frac{\partial \eta}{\partial t}+H\left(\frac{\partial u}{\partial x}+\frac{\partial v}{\partial y}\right)-\lambda\eta=0.$$

λ is adopted as 1/365 (day^{-1}). Additional runs were performed with λ of 1/30 (day^{-1}) and 1/10 (year^{-1}) to compare with λ of 1/365 (day^{-1}). These results showed that the time scale of spin-up and spin-down does not depend on the value of λ (not shown).

Case 3. Seasonal wind in winter

The seasonal wind near the Japan Sea is relatively strong in winter and is mainly from the northwest of the Japan Sea. The model was affected by the wind, which was taken to be 10 m/s over 90 days. The wind force factor was added to the eq. (1) and (2):

$$\frac{\partial u}{\partial t}-fv=-g\frac{\partial \eta}{\partial x}+A_h\left(\frac{\partial^2 u}{\partial x^2}+\frac{\partial^2 u}{\partial y^2}\right)-r_b\frac{u}{H}+\rho_a c_d W_x\sqrt{W_x^2+W_y^2}$$

$$\frac{\partial v}{\partial t}+fu=-g\frac{\partial \eta}{\partial y}+A_h\left(\frac{\partial^2 v}{\partial x^2}+\frac{\partial^2 v}{\partial y^2}\right)-r_b\frac{v}{H}+\rho_a c_d W_y\sqrt{W_x^2+W_y^2}$$

where ρ_a ($=0.0012\ \mathrm{g/cm^3}$) is air density, c_d ($=0.0013$) is the friction coefficient at the sea surface, and W_x, W_y ($=7.7\ \mathrm{m/s}$) are the x and y components of the northwesterly wind velocity ($=10\ \mathrm{m/s}$). In this case, assuming that the model ocean was closed, only the wind force factor was applied, without the in- and outflow.

Results

Time change of total kinetic energy

The time series of the basin-integrated kinetic energy was estimated to evaluate the steady state of flow pattern in each case (Fig. 5). It was found that the total

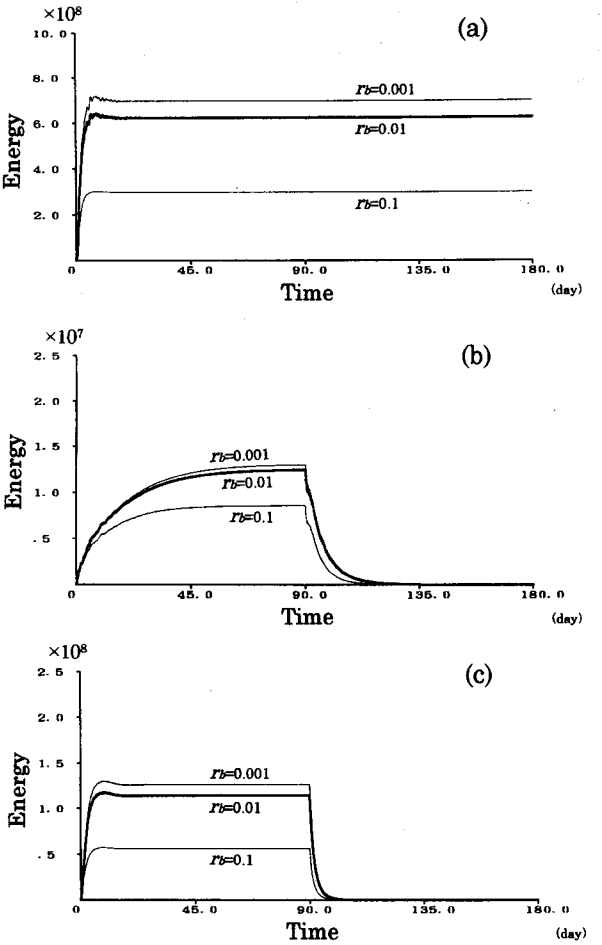

Fig. 5. The time series of the total kinetic energy for case 1(a), case 2(b) and case 3(c).

kinetic energy reached a statistical equilibrium by 30 days in cases 1 and 3, and by 60 days in case 2, and that the spin-up time did not depend on the value of the bottom friction coefficients (r_b).

In case 1, the total kinetic energy was consistent throughout integration, and this implied that there are currents in the model basin throughout the year. In contrast, in cases 2 and 3, the total kinetic energy dropped rapidly after 90 days. This corresponds to the time after which the forces in cases 2 and 3 were assumed to be zero. Moreover, at the 135 days there were no longer any currents. Thus, the simulated flows in cases 2 and 3 exist only in the winter.

It was considered that the time scale of the change of total kinetic energy might be governed by the propagation speed of some generated waves in all cases. In the following sections, therefore, the results will be concerned only with the results in the steady state using $r_b = 0.01$.

Case 1.

The velocity field at 90 days (steady state) is shown in Fig. 6(a). The water entering through the Tsushima Strait flows northeastward along the Japanese coast, and then it flows out through the Tsugaru Strait. The outflowing water through the Soya Strait comes mainly from the Russian coast.

Figure 6(b) shows the velocity field in the steady state in the vicinity of Cape

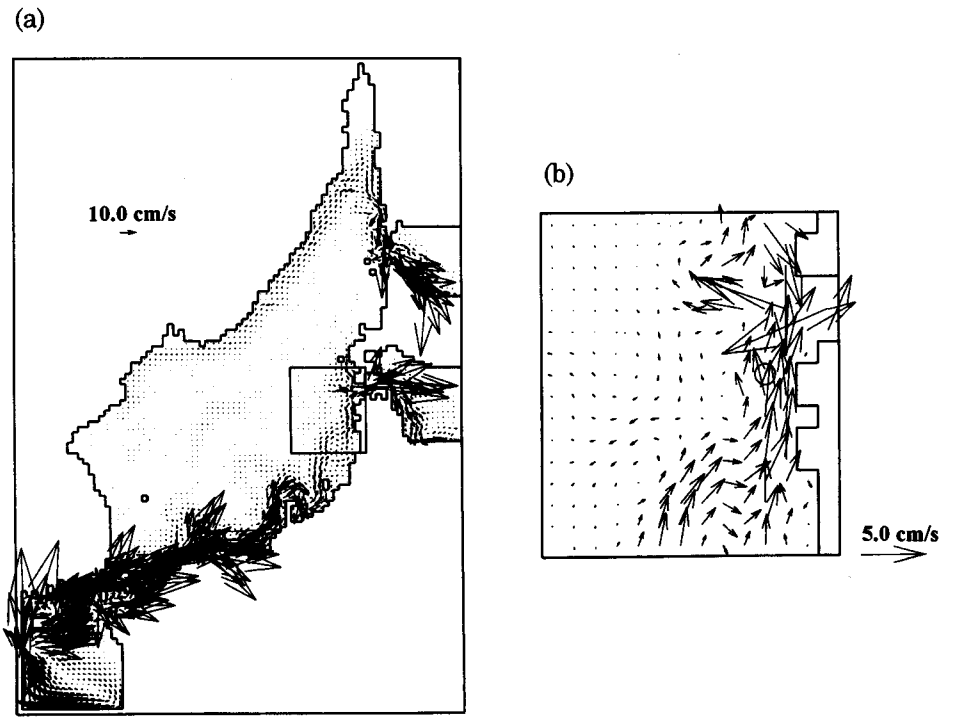

Fig. 6. The vector plots in the steady state increased by the forces of the in- and outflow for case 1(a), and the focused view in the vicinity of Cape Henashi (b). The symbol ○ corresponds to the location of the measurement point.

Henashi. The symbol ○ indicates the grid point corresponding to the measurement point. It is found that the anticyclonic gyre, is formed about 80 km offshore in the southward flow along the Hokkaido coast. At the measurement point, the current vector directed to the north and its magnitude was about 4.2 cm/s. The measured velocity was compared with the average velocity over the period of a year.

Case 2.

Figure 7(a) shows the velocity field at 90 days (steady state) in case 2. The water sinking off Vladivostok flows southwestward along the Russian coast, and then it splits into two branches near the west of the Yamato Rise : one branch flows along the Polar front and the other flows further to the south and northeastward along the Japanese coast. Then they rejoin each other near Cape Henashi.

The vector plot at the measurement point off Cape Henashi showed the northward flow but its magnitude (0.4 cm/s) was extremely small (Fig. 7(b)).

Case 3.

In the steady state, the pronounced northeastward flows are seen on both the Russian and the Japanese coasts, and there are few significant currents on other coasts (Fig. 8(a)). Most of the water which flows northeastward along the Russian coast flows out through the Soya Strait. It was also found that the outflowing water through the Tsugaru Strait comes from the north of the Tsugaru Strait as it flows southward along the Hokkaido coast.

Figure 8(b) shows the velocity field near Cape Henashi. The modeled vector plot at the measurement point indicated the flow was northward and that its

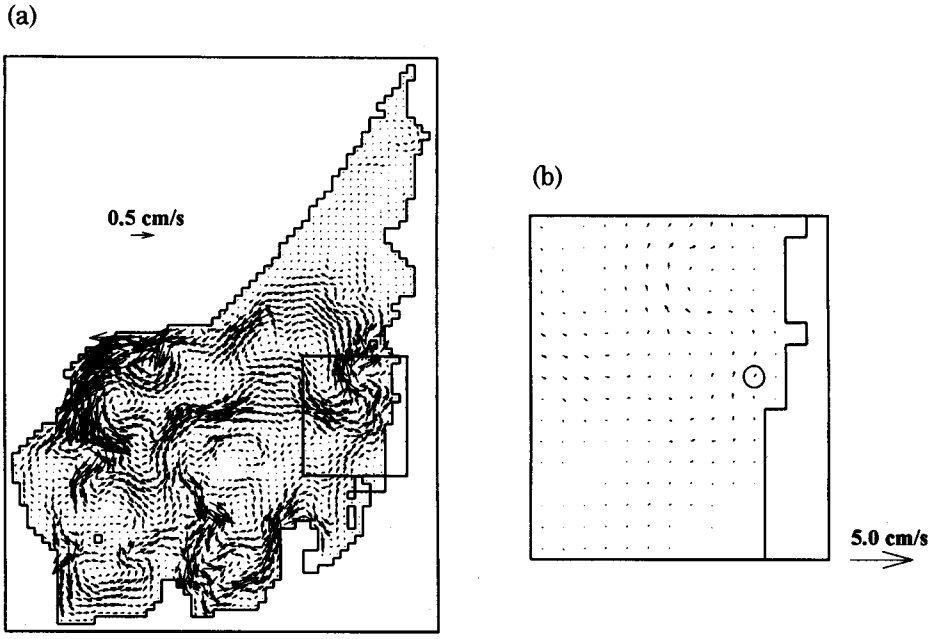

Fig. 7. Same as Fig. 6, but for case 2.

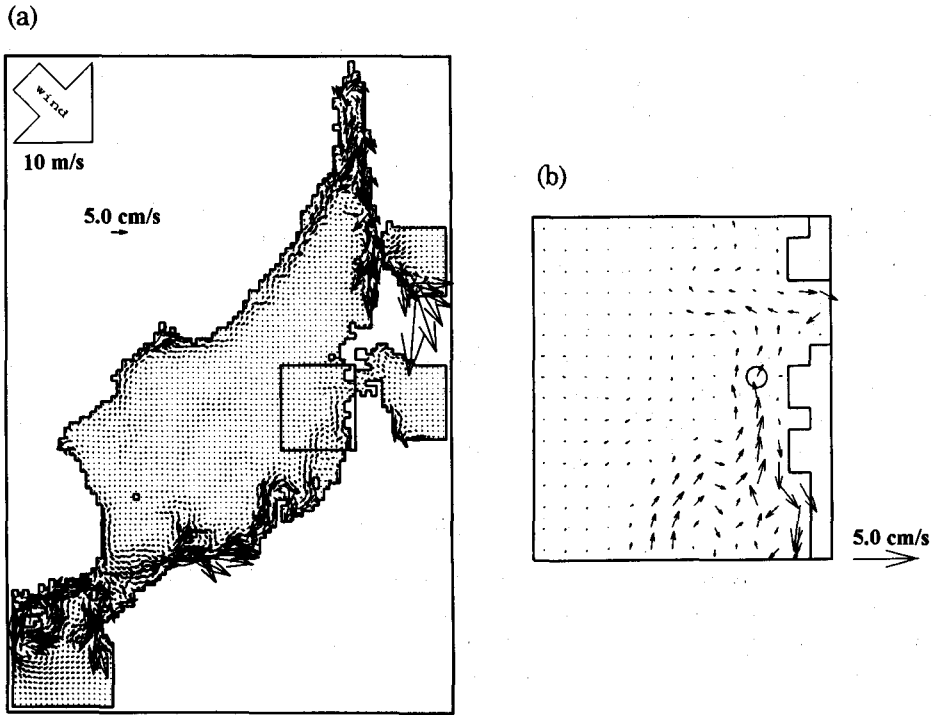

Fig. 8. Same as Fig. 6, but for case 3.

velocity was about 2.0 cm/s. It should be noted that the magnitude of the vector depended on the strength of the wind speed. With a wind speed of 20 m/s, the value of the vector was up to about 6.0 cm/s (not shown), which was compared with the observed one of 5.0 cm/s. However, as seen in the time series of the total kinetic energy (Fig. 5(b)), the northward flow existed only when wind stress was incorporated into the model.

Conclusion

In cases 1 and 3, the flow field reached an almost steady state by 30 days (Fig. 5(a)(c)). In case 2, on the other hand, it took about 60 days to become steady (Fig. 5(b)). This was due to the reduced gravity, g^*, which is about 1/300 of gravity acceleration (that is, a propagation speed of some generated waves which may govern the spin-up time.) The modeled flow fields came to rest immediately after the forces were eliminated in cases 2 and 3. Thus, the flow induced by the wintertime convection and the seasonal wind in winter does not exist throughout the year.

In cases 1 and 3 it was observed that the outflowing water through the Tsugaru/Soya Strait comes from the north. This might be because the Kelvin/Shelf wave generated near the Tsugaru/Soya Strait traveled with the coast to the right.

It was seen that the time change of measured current velocities vary within time periods of 10-20 days. To investigate such variations was outside the scope of this

study, but it is suggested that variation of the in- and outflow of the Japan Sea itself may cause such variation. Also, since it was found that the barotropic response is relatively sensitive to the wind forces, the wind forces are also the probable cause of the observed variation, but only in wintertime.

It is concluded that the probable cause of the relatively strong northward flow in the deep layer off Cape Henashi is the in- and outflow through the straits. As the study was concerned only with the barotropic response of the model, it is rather difficult to discuss quantitatively the results obtained. The influence of the surface layer circulation (for example, the Tsushima Warm Current and warm eddies) is important for the deep layer circulation of the Japan Sea.

It is considered that the result of this study is one of the causes of the deep flow off Cape Henashi. It is proposed that the simpler model's successes and failures to reproduce the observed dynamic features would be helpful in constructing a more complex model. It might be appropriate to consider applying the forces with variations, or using a more complex model.

Acknowledgments

We are greatly indebted to Prof. K. Ohtani and Mr. T. Murakami for providing the invaluable data relied upon for this research, and to Dr. M. Shimizu for the programming suggestions. We also wish to express our thanks to Ms. Helen M. Denny and Mr. Frank Denny for their careful reading of this manuscript.

References

Holloway, G., Sou, T. and Eby, M. (1995). Dynamics of Circulation of the Japan Sea. *J. Mar. Res.* **53**, 539-569.

Murakami, T., Nakayama, T., Isoda, Y. and Ohtani, K. (1995). Flow Structure of the Tsushima Warm Current off Cape Henashi, Aomori Prefecture. *Abstracts of the Spring Convention in 1995 the Oceanogr. Soc. of Japan*, pp. 219-220 (in Japanese).

Senjyu, T. and Sudo, H. (1994). The Upper Portion of the Japan Sea Proper Water ; Its Source and Circulation as Deduced from Isopycnal Analysis. *J. Oceanogr.* **50**, 663-690.